Process Intensification for the Recovery of Hydrogen Cyanide in the Andrussow Process

Luca Lehrich and Chafika Adiche*

DOI: 10.1002/cite.202200059

Supporting Information available online

The aim of this work was to determine a cost-optimal design of the distillation unit of the Andrussow process. For this purpose, a feed with a mass flow rate of 121 t h^{-1} and a concentration of ca. 2 wt % hydrogen cyanide (HCN) was considered. An approach for a cost-optimal process intensification was developed with the goal to achieve the desired product qualities, while minimizing the organonitrile accumulation in the column. For this purpose, the simple distillation column of the established cost-optimal design of the base case was extended to a configuration with a side stripper with taking into consideration heat integration in the process. It was found that this new configuration allows a much smaller accumulation of organonitriles in the main column; reducing thereby the operation issues of the process while decreasing considerably the total annual cost of the distillation unit by 61 % as compared to that of the base case design.

Keywords: Andrussow process, Cost model, Distillation process, Heat integration, Organonitrile contaminants, Process intensification

Received: May 16, 2022; *revised:* September 11, 2022; *accepted:* October 26, 2022

1 Introduction

Hydrogen cyanide (HCN) is a key intermediate for the production of a wide range of products including plastics (e.g., Plexiglas®), construction chemicals, coatings adhesives, pharma products, synthetic fibers, herbicides, amino acids (methionine), chelating agents and sodium cyanide. In reason of its hazardous and toxic properties, HCN is generally converted into the target product on site. Among the several processes developed for HCN manufacturing, the Andrussow process [1, 2] is the most widely used synthesis route (Fig. 1). Accordingly, hydrogen cyanide is produced in gas phase from methane (CH_4), ammonia (NH_3) and compressed oxygen (from air) using a platinum gauze catalyst for a temperature greater than 1000 °C and at around atmospheric pressure [3] so that

$$CH_4 + NH_3 + 1.5O_2 \rightarrow HCN + 3H_2O, \quad \Delta H_R = -474\ \text{kJ/mol} \tag{1}$$

A detailed description of the Andrussow process can be found elsewhere [3–5].

As main source of methane, the natural gas used as raw material for the Andrussow process contains besides methane higher hydrocarbons (impurities) like ethane and propene. The latter are converted during the reaction step into organonitriles such as acetonitrile and acrylonitrile [6]. It

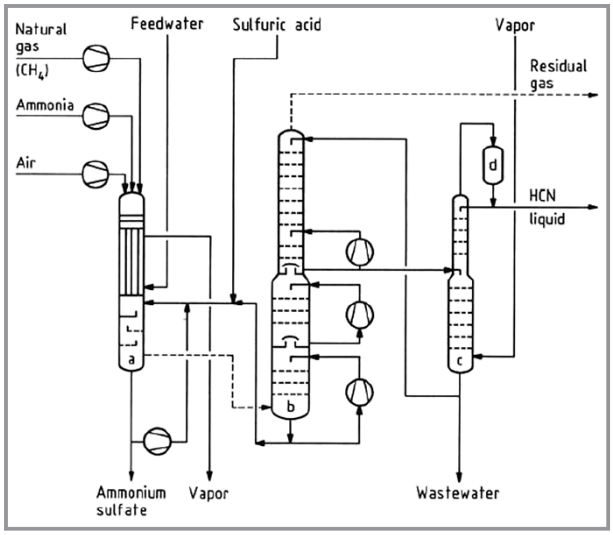

Figure 1. Simplified diagram of the Andrussow process [3]: a) reactor and ammonia scrubber, b) HCN absorption tower, c) HCN rectifier, d) condenser.

Luca Lehrich,
Dr.-Ing. Chafika Adiche https://orcid.org/0000-0002-9371-8139 (c.adiche@outlook.de)
Technische Universität Darmstadt, Department of mechanical engineering, Thermal Process Engineering Group, Otto-Berndt-Straße 2, 64287 Darmstadt, Germany.

results that the feed to the distillation column (bottom product of the HCN absorber) is a dilute aqueous solution of HCN containing organonitrile contaminants. The concentration of organonitriles in the column can increase to a level; leading to their polymerization and inducing thereby the polymerization of HCN [6, 7], which rate can be increased further under alkaline condition (presence of unreacted ammonia in the process streams) and with temperature rising [3]. To stabilize the hydrogen cyanide in the process, small amounts of sulfuric or phosphoric acids and sulfur dioxide are usually added to the liquid and vapor phases, respectively; acting thereby as polymerization inhibitors for high HCN concentration [3] and also to minimizing the HCN dissociation and loss in the bottom product where a very low HCN concentration is prevailing [8]. In fact, the polymerization of HCN and organonitriles causes fouling of mass transfer equipment (e.g., tray clogging) and blocking or plugging of plant pipelines by polymer. That leads to the decrease of the separation efficiency of the column and thus to lower HCN yield. Furthermore, it can also present a hazard to the operating personnel and to the environment, since overpressures (e.g., of HCN in gaseous form) can occur, resulting thereby in leakage points (due to blowouts of gaskets), which can lead to the release of the toxic HCN into the environment [6]. In addition to that, the accumulation of organonitriles (e.g., acrylonitrile) in the column can lead to the apparition of foaming due to the tendency of such mixtures to form two liquid phases (e.g., water-rich and acrylonitrile-rich phases) [7]. To overcome the above mentioned issues, the column must periodically be purged, otherwise column performance deteriorates and the risk to get a poor quality product or process upsets increases [7]. This purge will result in a loss of HCN production. Furthermore additional costs due to additional purification steps and to equipment maintenance downtime for cleaning are required.

The aim of this work was to develop an intensification approach of the distillation unit in the Andrussow process that

1) allows the minimization of the build-up of organonitrile contaminants in the column,
2) fulfills the column performance (product qualities) and
3) provides a cost-optimal design with an energy efficient process configuration.

2 Thermodynamic Model

In fact, the stream entering in the distillation column of the Andrussow process contains in addition to a dilute aqueous solution of HCN and organonitriles also small amounts of acids (e.g., H_2SO_4) and non-condensable gases (H_2, N_2, CO, O_2, CH_4, CO_2, unreacted NH_3, SO_2). In this work, we have focused our investigations on the development of a cost-optimal and energy efficient design of the distillation unit of the Andrussow process with taking into account the minimization of the accumulation of organonitrile contaminants in the column. For this purpose, and at this conceptual design stage, we have assumed that acids and non-condensable gases are not present in the feed stream. Consequently, the feed of the distillation unit of the Andrussow process considered in this work is a dilute aqueous mixture, which only contains hydrogen cyanide, acrylonitrile and acetonitrile.

In fact, the main separation task of the distillation column is the recovery of HCN as distillate product with a purity $\geq$ 99.5 wt % from a dilute aqueous solution (see also Sect. 3). So, let us first examine the behavior of the thermodynamic phase equilibrium of the binary system constituted by HCN and water. In addition to the polar nature of this mixture, hydrogen cyanide is a weak volatile electrolyte (weak acid) [8]. Mixed with water, it partially dissociates into cyanide- and hydronium ions. The electrolyte dissociation increases with the concentration decrease of HCN in water until reaching a complete dissociation at infinite dilution [8]. While HCN is volatile in its molecular form, its ions can evaporate only at very high temperature [8]. It results that for the considered temperature range for this process ($\leq$ 100 °C), the vapor phase dissociation is neglected.

Accordingly, two thermodynamic models which may be appropriate for the description of the thermodynamic phase equilibrium of this system were considered in this work:

1) regressed NRTL model, using binary interaction parameters obtained by regression of appropriate experimental phase equilibrium data. For this purpose, the regression tool of *Aspen Plus V11* with a *4-parameter maximum likelihood approach* was used to fit the selected experimental data sets (at isobaric condition) from the *NIST* databank available in Aspen Plus V11 and
2) ELECNRTL model (appropriate for electrolyte systems), with using the databank APV110 ENRTL-RK (available in *Aspen Plus V11*) for the prediction of the Henry constant and the binary and electrolyte pair parameters.

Fig. 2 illustrates the experimental liquid-vapor equilibrium curves of the system HCN-water and those obtained by the two above-mentioned thermodynamic models. It is shown that the phase equilibrium curves obtained by the regressed NRTL model present a quite good agreement with the respective experimental data. Let us now compare between the phase equilibrium data obtained by the regressed NRTL and the ELECNRTL models. Fig. 2 shows that the dew point curves for both models almost coincide with each other. That can be attributed to the fact that in the gas phase only molecular HCN is present and subject to condensation. On the other side, if the bubble point curves of these two models are compared, we can see that the ELECNRTL model predicts moderately greater bubble point temperatures in the composition range between ca. 0.05 and 0.8. That can be explained by the fact that with the decrease of HCN concentration in the aqueous mixture, the concentrations of its non-volatile ions become relatively greater, leading therefore to higher bubble point temperatures as

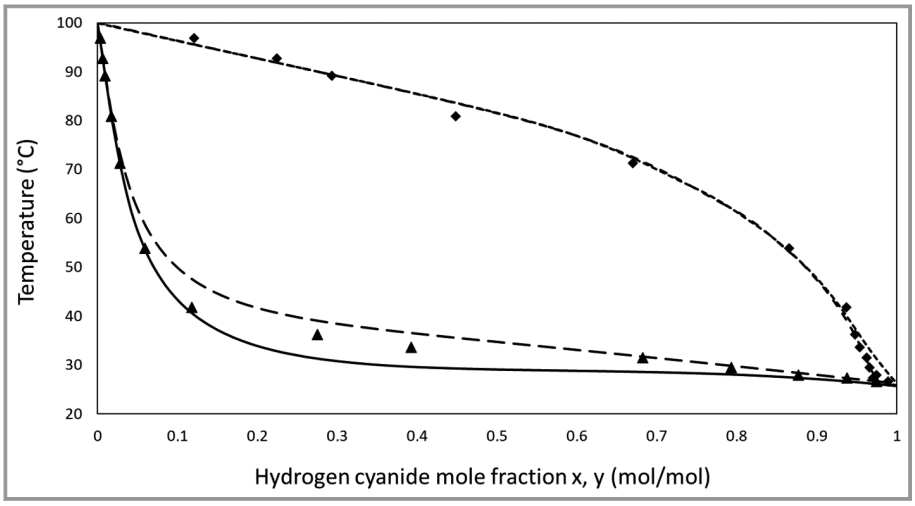

Figure 2. Phase equilibrium curves of the binary mixture of hydrogen cyanide and water using different thermodynamic models. - - - Dew point curve, ELECNRTL model; – – dew point curve, regressed NRTL model; ◆ experimental dew point curve [9]; – - bubble point curve, ELECNRTL model; — bubble point curve, regressed NRTL model; ▲ experimental bubble point curve [9].

compared to those obtained for the same mixture compositions by the regressed NRTL model, for which no HCN dissociation is taken into account. Finally, Fig. 2 shows that the phase equilibrium curves determined by the regressed NRTL model present a better agreement with the experimental data than those obtained by the ELECNRTL model. It is particularly the case for a mixture composition close to unity (pure HCN), where a tangential azeotrope is identified by both the experimental phase equilibrium data and by the phase equilibrium curves of the regressed NRTL model. According to the latter, Fig. S1 in the Supporting Information (SI) shows that the tangential azeotrope of the system HCN-water occurs at a mole fraction of ca. 0.996, which corresponds to a mass fraction of 0.9972. The latter is, however, greater than the distillate product purity specified for the design of the distillation unit of the Andrussow process (see Sect. 3) and has therefore no negative impact on the satisfaction of the desired distillate product quality for the investigated process in this work.

Based on the previous analysis, the regressed NRTL model was selected in this work to describe the thermodynamic phase equilibrium behavior of the HCN-water system and of the remaining binary systems constituting the feed of the distillation column of the Andrussow process. Also, for each of these binary systems, an appropriate experimental data set (at isobaric condition) was selected from the *NIST* databank (in Aspen Plus V11) and the same above-mentioned regression approach was successfully applied (Fig. 3). Accordingly, it was found that the mixture of acrylonitrile and water builds a heterogeneous temperature minimum azeotrope (Fig. 3a), whereas the mixture of acetonitrile and water forms a homogenous temperature minimum azeotrope (Fig. 3b). The two organonitriles constituted by acetonitrile and acrylonitrile form a close boiling point system due to their nearly similar structure, which leads to a difficult separation between them (Fig. 3c). And finally, both binary systems HCN-acrylonitrile and HCN-acetonitrile exhibit a nearly ideal thermodynamic behavior as depicted in Figs. 3d and 3e, respectively.

3 Cost-Optimal Design of the Distillation Unit of the Base Case

Fig. 4 illustrates the distillation unit of the Andrussow process investigated in this work. The distillation unit is operating at atmospheric pressure and allows the recovery of HCN from a dilute aqueous feed according to the design specifications provided in Tab. 1. For the design of the base case, we consider that the product of the absorber of the Andrussow process is a binary mixture of HCN and water with a temperature of 20 °C, a mass flow rate of 121 000 kg h^{-1} and a HCN mass concentration of 2.1 wt %; corresponding therefore to a process capacity of ca. 2540 kg h^{-1} HCN, which is a typical capacity of a commercial plant [3]. This stream is then heated up to a temperature of 75 °C and introduced as feed into the simple distillation column. It should be noticed that the selected temperature of the preheated feed is ca. 10 °C smaller than that of the saturated liquid mixture (i.e., the feed is introduced into the column at subcooled condition). That permits to diminish the impact of the corrosive process stream (which actually contains small amounts of strong acids) [3–5] on the equipment corrosion, which rate tends to increase with rising temperature [15].

Table 1. Design specifications of the distillation unit of the Andrussow process.

	Distillate product	Bottom product
Mass flow rate [kg h^{-1}]	ca. 2540	–
Hydrogen cyanide	min. 99.5 wt %	max. 140 ppmw
Total carbons	–	max 500 ppmw

Furthermore, to prevent the corrosive impact of the process streams on the distillation unit, stainless steel 1.4301 [16] was selected as material of construction for the whole plant (including column vessel(s), mass transfer equipment and heat exchangers). Also, sieve trays were selected for the distillation column to better counteract the fouling issues caused by polymerization and the effects of corrosion [17].

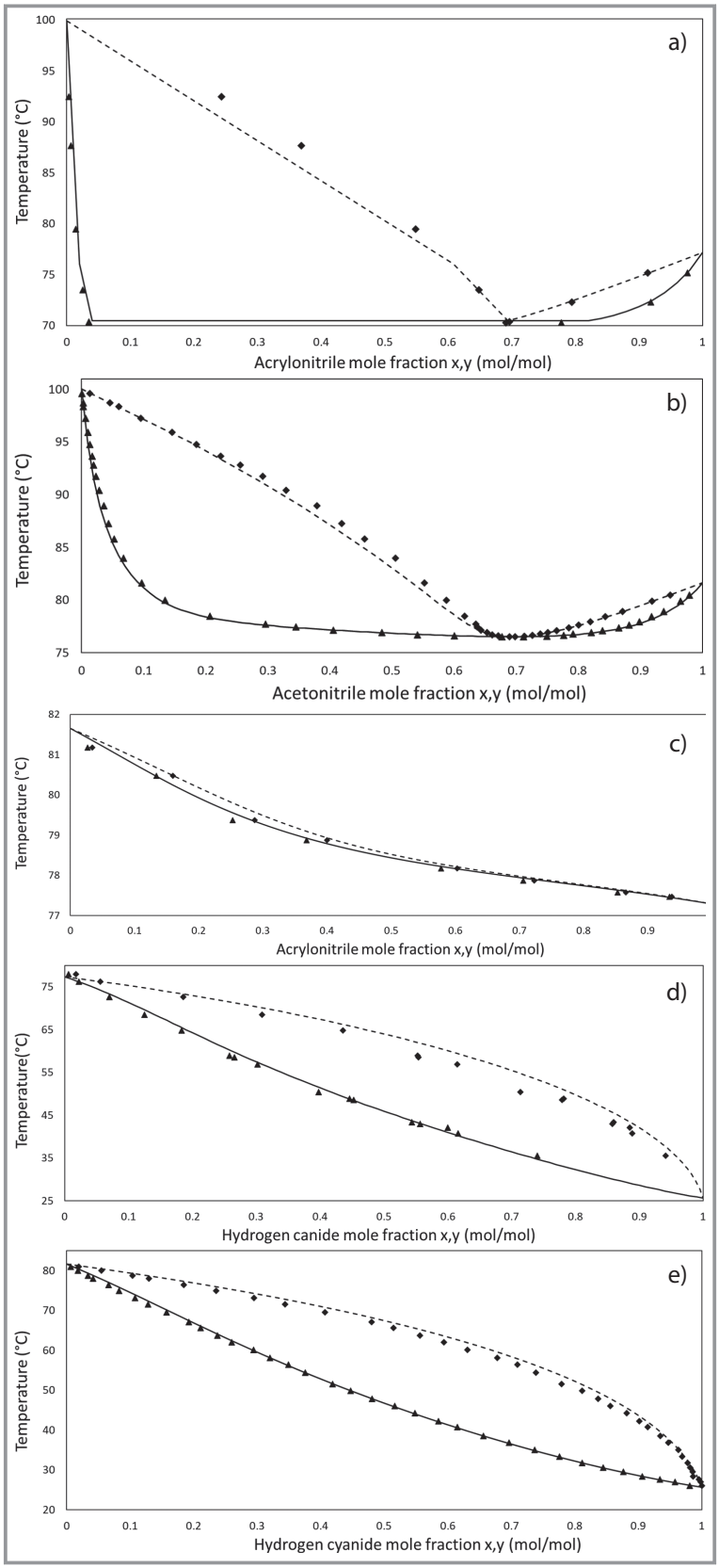

3.1 Cost Model

In the following sections, we will deal with the design optimization of the distillation unit of the Andrussow process. For this purpose, the minimization of the total annual cost (*TAC*) of the investigated process was selected as economic objective function. The latter is useful and commonly used for design optimization purpose and for screening of different process alternatives at the conceptual design stage [18]. Accordingly, the *TAC* of the distillation unit is determined as follows

$$TAC = C_{cap}/t_{pb} + t_{op}C_{op} \tag{2}$$

The operating cost C_{op} includes the utility (energy) costs of the low-pressure water steam (lp-steam) C_{lps} at the reboiler(s) and the heat exchanger for the feed preheating and of the chilled water C_{cw} at the condenser and is given by

$$C_{op} = C_{lps} + C_{cw} \tag{3}$$

with

$$C_{lps} = 3600(Q_{reb} + Q_{hex})C_{lps/j} \tag{4}$$

and

$$C_{cw} = 3600Q_{cond}\, C_{cw/j} \tag{5}$$

where t_{op} is the operation time of the plant and is given by a value of 8000 h a^{-1} and t_{pb} is the payback period of the distillation plant and is given by 3 years. Prices and properties of heating and cooling media are provided in Tab. S1 (SI). The installed equipment cost C_{cap} includes the purchased prices for the column vessel and trays, reboiler, condenser including the feed preheater. It takes into consideration the inflation between 2003 and 2019 and is given by

$$C_{cap} = 4(CEPCI_{2019}/CEPCI_{2003})\,(C_{col} + C_{cond} + C_{reb} + C_{hex}) \tag{6}$$

Figure 3. Experimental and predicted thermodynamic phase equilibrium curves (regressed NRTL model) of the binary systems: a) acrylonitrile-water, b) acetonitrile-water, c) acrylonitrile-acetonitrile, d) hydrogen cyanide-acrylonitrile, e) hydrogen cyanide-acetonitrile. - - - Dew point curve, regressed NRTL model; — bubble point curve, regressed NRTL model; ◆ experimental dew point curve a) [10], b) [11], c) [12], d) [13], e) [14]; ▲ experimental bubble point curve a) [10], b) [11], c) [12], d) [13], e) [14].

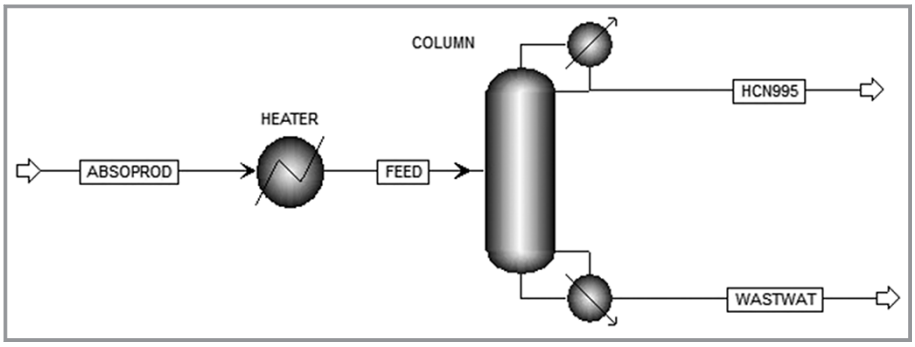

Figure 4. Simplified process flowsheet of the base case.

where C_{col}, C_{cond}, C_{reb} and C_{hex} are the purchased prices of the column vessel and trays, the condenser, the reboiler and the preheater in the year 2003, respectively (SI Tab. S2). $CEPCI_{2019}$ and $CEPCI_{2003}$ are equal to 607.5 and 402, respectively. The cost correlations are taken from reference [19]. For the capital cost estimation, the column diameter D and column height H were obtained for given design specifications by using the *Aspen Tray Sizing tool (Aspen Plus V11)* for a column design at 75 % of flooding point [17]. Whereas, the column vessel weight W and the surface area of the heat exchangers ($A_{reb,mc}$, A_{cond} and A_{hex}) were determined by the *Aspen Process Economic Analyzer (APEA) (Aspen Plus V11)*.

3.2 Design Optimization of the Distillation Column of the Base Case

A design procedure of the distillation column of the base case was developed similarly to the optimization approach presented in [20] and can be summarized in the following steps:

1) Determine initial design estimates of the distillation column by *DSTWU (Aspen Plus)* for the specified product purities (Tab. 1).
2) Carry out a first column simulation with *Radfrac model (Aspen Plus)* using the initial design estimates obtained by DSTWU (total number of theoretical stages N_T, feed stage and reflux ratio RR). An overall stage efficiency of 0.6 is used. The latter is appropriate for design purpose [17] and is applied for all column simulations.
3) Implement two design specification blocks for product purities using the *Aspen Plus Design specification tool (Aspen Plus)*. The latter adjusts the reflux ratio and distillate flow rate in order to achieve the specified product purities.
4) Determine the optimal feed stage location N_F corresponding to the minimum reboiler heat duty $Q_{reb,mc}$ by using the *Sensitivity Model Analysis Tool (Aspen Plus)*.
5) Calculate the TAC of the distillation column.
6) Increase N_T and repeat steps 3 to 5 until the column with the minimum TAC is found.

Six design scenarios with N_T equal to 16, 18, 20, 22, 24, and 26 were selected. Tab. 2 summarizes their respective optimal design parameters and capital, annual energy and total annual costs. It was found that the minimum TAC corresponds to a total number of theoretical stages N_T equal to 22, which corresponds to a reflux ratio RR of 1.33 and a number of sieve trays of 37. In the following discussion, this design scenario will be designated as the cost-optimal design of the base case. If we consider additionally, the feed preheater using low pressure steam (lp-steam) as heating medium, then the annual utility cost for this process will increase by a value of 2 725 030 € a^{-1}, the capital cost by a value of 166 092 €, resulting therefore in an increase of the TAC by a value of 2 780 394 € a^{-1}. Tab. 3 summarizes the design and operating parameters obtained for the cost-optimal design of the base case including the distillation column and the feed preheater.

4 Influence of Organonitrile Contaminants in the Feed

In this section, we examine the influence of the concentration of organonitriles in the feed (e.g., acrylonitrile and acetonitrile) on the separation performance of the distillation column of the cost-optimal base case with the previously

Table 2. Screening of several design scenarios of the simple distillation column of the base case for design optimization.

N_T	N_F [a)]	RR	Annualized utility cost [€ a^{-1}]	Capital cost €	TAC [€ a^{-1}]
16	9	2.16	2 258 445	1 921 502	2 898 946
18	9	1.66	2 075 112	1 927 033	2 717 457
20	9	1.45	1 995 438	1 983 877	2 656 730
22	10	1.33	1 949 752	2 043 653	2 630 969
24	10	1.27	1 928 282	2 116 016	2 633 621
26	10	1.24	1 919 863	2 191 145	2 650 245

a) Count the number of theoretical stages in the column by starting with the first stage at the top of the column.

Table 3. Cost-optimal design and operating parameters of the base case

Distillation column	Value
Number of trays	37
Reflux ratio *RR*	1.33
Distillate flow rate [kg h^{-1}]	2537.1
Column diameter *D* [m]	1.62
Column height *H* [m]	*13.41*
Tray type	Sieve trays
Material of construction (trays and column shell)	Stainless steel 1.4301, AISI 304
Reboiler	
$Q_{reb,mc}$ [J s^{-1}]	4 879 303.89
$A_{reb,mc}$ [m^2]	130.46
Material of construction	Stainless steel 1.4301, AISI 304
Condenser	
Q_{cond} [J s^{-1}]	–1 634 272.51
A_{cond} [m^2]	99.25
Material of construction	Stainless steel 1.4301, AISI 304
Feed preheater (using lp-steam)	
Q_{hex} [J s^{-1}]	8 127 401.68
A_{hex} [m^2]	73.52
Material of construction	Stainless steel 1.4301, AISI 304

obtained operating parameters (reflux ratio and distillate product (see Tab. 3). For this purpose, we have considered three feed compositions (Tab. 4). Tab. 4 shows that for all three investigated feed compositions, the minimum required purity of hydrogen cyanide in the distillate (99.5 wt %) could not be reached. Furthermore, the maximum value of mass fraction of hydrogen cyanide allowed in the bottom (140 ppmw) was exceeded in all three cases, whereas the maximum allowed amount of total carbon in the bottom product (500 ppmw) was only exceeded for the feed composition of the third case.

4.1 Impact on the Column Capacity

The following sections will deal with the analysis and design calculations of the distillation unit for the feed composition of the 2nd case. Similar investigations can also be conducted for both other feed compositions. Starting with the operating parameters of the distillation column of the cost-optimal design of the base case, the reflux ratio has been

Table 4. Influence of organonitrile concentration in the feed on the separation performance of the distillation column of the cost-optimal base case design.

Feed	Mass fraction		
	1st case	2nd case	3rd case
Hydrogen cyanide	0.021	0.021	0.021
Acrylonitrile [ppmw]	100	100	100
Acetonitrile [ppmw]	300	600	900
Water	0.9786	0.9783	0.9780
Distillate			
Hydrogen cyanide	0.987714	0.986820	0.985243
Acrylonitrile	0.004768	0.004768	0.004768
Acetonitrile	0.000036	0.000146	0.000442
Water	0.007483	0.008266	0.009547
Bottom product			
Hydrogen cyanide [ppmw]	296	315	349
Acrylonitrile [ppbw]	26	22	23
Acetonitrile	0.000305664	0.000609730	0.000909815
Water	0.999398258	0.999075056	0.998741200
Total carbon [ppmw]	310	497	687

increased in order to achieve the required product specifications (Tab. 1). Tab. 5 shows that as compared to the feed with the binary mixture of HCN and water, the presence of organonitrile contaminants in the feed (2nd case) leads as expected to a substantial increase of the reflux ratio in the column up to a value of 7.8. This results in a significant increase of liquid load in the column, which can rapidly lead to column overloading and flooding [17]. To deal with this issue, the design of the simple column of the cost-optimal base case design was modified. The new design of the simple column (also carried out at 75 % of flooding point) provides for the same total number of theoretical stages (and also for the same column height), a column diameter of 2.32 m instead of 1.62 m for the cost-optimal design of the base case. Furthermore, and as compared to the latter, the modified design gives rise to almost four times greater

Table 5. Comparison of the operating conditions for the simple column of the cost-optimal base case design with and without organonitrile contaminants in the feed.

Parameter	Feed without organonitriles	Feed with organonitriles (2nd case)
Reflux ratio *RR* [–]	1.33	7.8
$Q_{reb,mc}$ [J s^{-1}]	4 879 303.89	9 391 193.84
Q_{cond} [J s^{-1}]	–1 634 272.51	–6 182 409.53

heat exchange area for the condenser, two times larger heat exchange area for the reboiler and 1.2 times larger heat exchange area for the preheater (Tab. 6).

4.2 Impact on the Organonitrile Composition Profiles in the Column

Another issue of the presence of organonitrile contaminants in the feed (2nd case) is their accumulation in both the liquid and vapor phases along the column height. Fig. 5 shows that the highest organonitrile concentrations (here of acrylonitrile) accumulated in the liquid and vapor phases, correspond to mass fractions up to 0.708 and 0.710, respectively. These values are reached at stage 9 (rectifying section) and at stage 16 (stripping section), respectively. As mentioned previously in the introduction section, that can result in the polymerization of organonitriles and HCN, and to foaming apparition in the column due to liquid phase separation (i.e., formation of water-rich and acrylonitrile-rich liquid phases) [7].

Table 6. Results of the modified design of the simple distillation column with a preheater based on the feed composition of the 2nd case.

Distillation column	Value
Column diameter D [m]	2.32
Column height H [m]	13.41
$A_{reb,mc}$ [m^2]	246.40
A_{cond} [m^2]	376.51
Feed preheater (using lp-steam)	
A_{hex} [m^2]	85.83

5 Design Approach for Process Intensification

5.1 Integration of a Side Stripper

To minimize the accumulation of organonitriles in the distillation column, the simple column of the cost-optimal

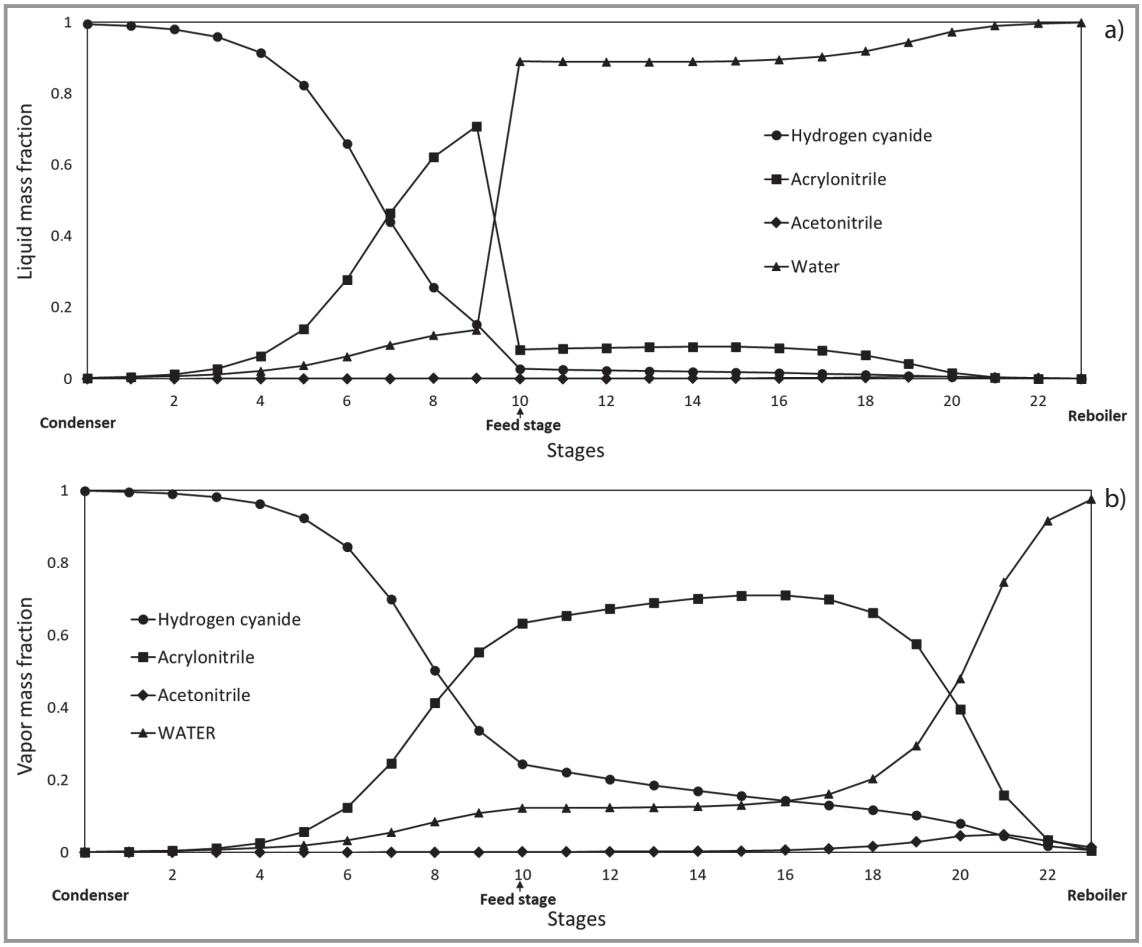

Figure 5. Component mass fraction profiles in the simple distillation column of the base case with modified design (Tab. 6) for a) the liquid phase, b) the vapor phase.

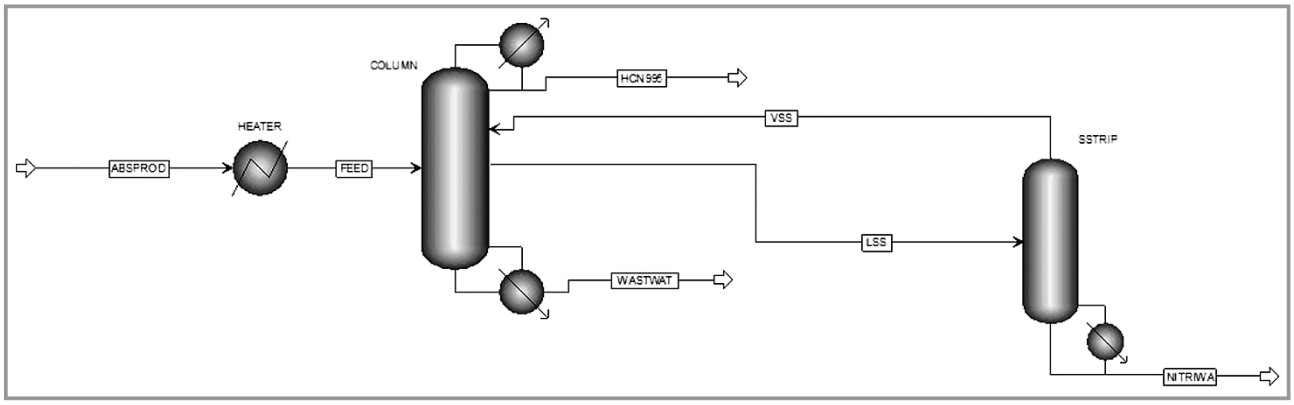

Figure 6. Extension of the simple column of the cost-optimal design of the base case to a column with a side stripper.

design of the base case was extended to a column with a side stripper (Fig. 6). The design of such column configuration (column with a side stripper) requires four additional design specifications: two design parameters, which are the side stream stage and the number of theoretical stages in the side stripper and two operating parameters, which are the mass flow rates of the side stream (L_{ss}) and of the bottom product of the side stripper *(NITRIWA)* [21, 22]. Furthermore, the reflux ratio of the main column has to be adjusted to achieve the desired product qualities.

Let us examine the liquid phase composition profile of organonitriles (here acrylonitrile) in the main column (Fig. 5). We can see that the stages 6 to 9 in the main column seem to be potential candidates for the location of the side stream withdrawal. For a given side stream stage, e.g., stage 8 (stage numbering is started at the first stage at the top of the column), a first design estimation of the side stripper was established by process simulation for L_{ss} = 1000 kg h^{-1}, *NITRIWA* = 500 kg h^{-1} and four theoretical stages in the side stripper. That corresponds also to a reflux ratio of 1.85 in the main column and maximum mass fractions of organonitriles (acrylonitrile and acetonitrile) in the main column of 0.0566 and 0.059 in the liquid and vapor phase, respectively (see SI Tab. S3). To decrease further the latter (i.e., the liquid and vapor mass fraction of organonitriles in the main column), additional design simulations were carried out with keeping this time *NITRIWA* equal to 500 kg h^{-1} and by increasing gradually L_{ss} up to a value of 1900 kg h^{-1}. Note that for all performed design simulations, the desired product specifications were achieved and liquid phase separation in the liquid side stream was not obtained.

Fig. 7 shows that among the simulated design cases, that case with L_{ss} = 1700 kg h^{-1} and *NITRIWA* = 500 kg h^{-1} results in a minimum value of the maximum concentration

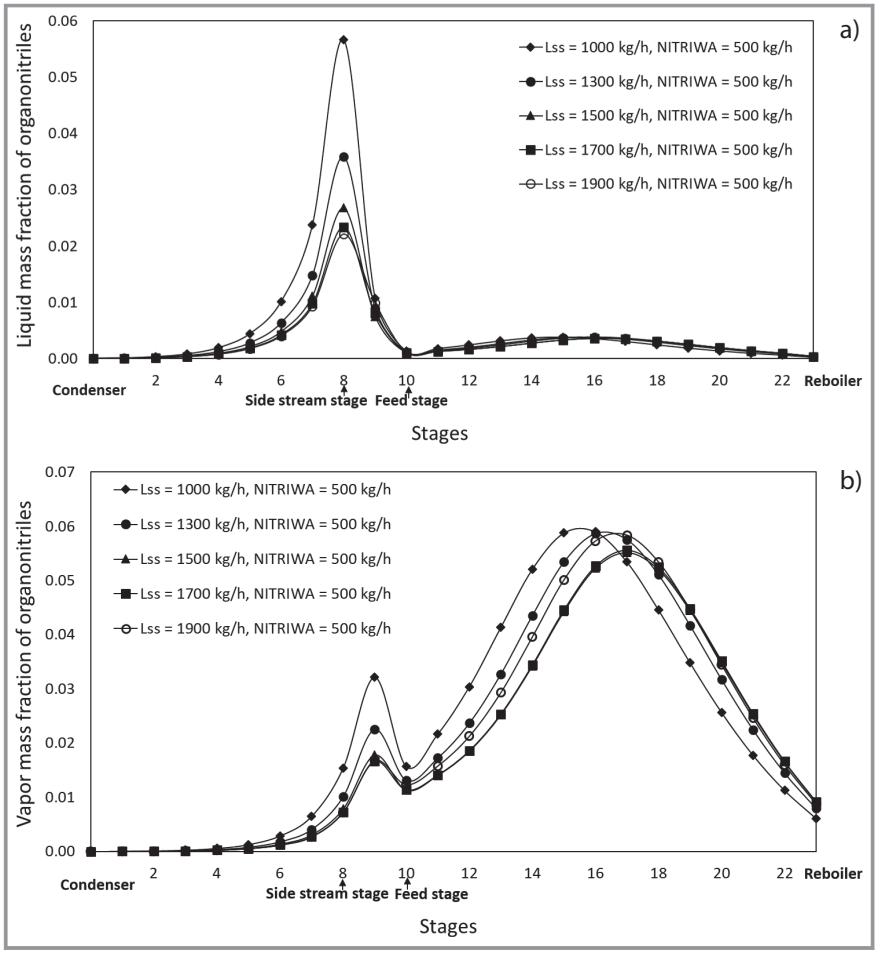

Figure 7. Influence of the mass balance in the side stripper on a) the liquid composition profile of organonitriles in the main column, b) the vapor composition profile of organonitriles in the main column.

of organonitriles in the main column for both liquid and vapor phases (see SI Tab. S3). Tab. 7 summarizes the obtained mass balance data of the new established design of the distillation unit, for which a HCN loss of 0.45 wt % was obtained. Furthermore, the optimal number of theoretical stages in the side stripper determined for this design case was 8.

The above-mentioned investigations have been also carried out for the other side stream withdrawal location candidates and the stage 8 in the main column was found to be the optimal liquid side stream location. Furthermore, and as compared to the cost-optimal design of the base case (with the simple column), the reflux ratio in the main column for this new design configuration (column with a side stripper) was decreased to a value of 1.93 instead of 7.8, avoiding thereby the overloading and flooding of the main column.

When comparing the composition profiles of organonitriles in the main column before the side stripper integration (Fig. 5) with those after the side stripper integration (Fig. 8), it can be well seen that their accumulation has been significantly declined along the main column and in both phases; reducing therefore the risk of polymerization, foaming and column overloading.

Based on the obtained optimal conditions of the established design of the Andrussow distillation column with an integrated side stripper, the latter (the side stripper) was designed at 75 % of flooding point using an appropriate design procedure [17] and packing data provided in reference [23]. The obtained design parameters of the side stripper are summarized in Tab. 8.

Finally, Tab. 9 shows that as compared to the distillation unit of the base case with the modified design of the simple column (Tab. 6), the new established design with a column with a side stripper permits both capital and annual energy costs savings; leading therefore to a decrease of the *TAC* by 30 %.

Table 8. Design parameters of the side stripper.

Parameter	Value
Packing type	Mellapack Sulzer 250Y
Column diameter [m]	0.47
Column height [m]	3.04
Material of construction (column vessel and packing)	Stainless steel 1.4301, AISI 304
Reboiler	
$Q_{reb,ss}$ [J s^{-1}]	330 250.48
$A_{reb,ss}$ [m^2]	5.56
Material of construction	Stainless steel 1.4301, AISI 304

Table 9. Impact of design configuration on the annual energy, capital and total annual costs.

	Distillation unit	
	simple column with modified design	simple column of the cost-optimal design of the base case with integrated side stripper
Reflux ratio in the main column [–]	7.8	1.93
Q_{reb} [J s^{-1}]	9 391 193.84	5 277 304.76
Q_{cond} [J s^{-1}]	–6 182 409.53	–2 058 637.34
Annualized utility costs[a)] [€ a^{-1}]	7 060 288	4 889 181
Capital cost[a)] €	3 622 363	2 624 088
Total annual costs[a)] [€ a^{-1}]	8 267 742	5 763 877

a) Preheating with lp-steam is included.

Table 7. Mass balance of the column with a side stripper for L_{ss} = 1700 kg h^{-1} and *NITRIWA* = 500 kg h^{-1}.

	Feed	HCN995	WASTWAT	L_{SS}	V_{SS}	*NITRIWA*
Mass flow rate [kg h^{-1}]	121 000	2537.1	117 962.9	1700	1200	500
HCN	2541.00	2529.66	10.75	1172.56	1171.98	0.58
Acrylonitrile	12.10	0.02	0.00	12.55	0.46	12.09
Acetonitrile	72.60	0.04	46.59	27.23	1.26	25.97
Water	118 374.30	7.38	117 905.56	487.66	26.30	461.36
Mass fraction						
HCN	0.021	0.9971	$9.11 \cdot 10^{-5}$	0.6897	0.977	0.0012
Acrylonitrile	0.0001	$6.01 \cdot 10^{-6}$	$8.53 \cdot 10^{-10}$	0.0074	$3.84 \cdot 10^{-4}$	0.0242
Acetonitrile	0.0006	$1.53 \cdot 10^{-5}$	0.0004	0.0160	0.0011	0.0519
Water	0.9783	0.0029	0.9995	0.2869	0.0219	0.9227
Total carbon	0.0098	0.4431	0.0003	0.3209	0.4349	0.0473

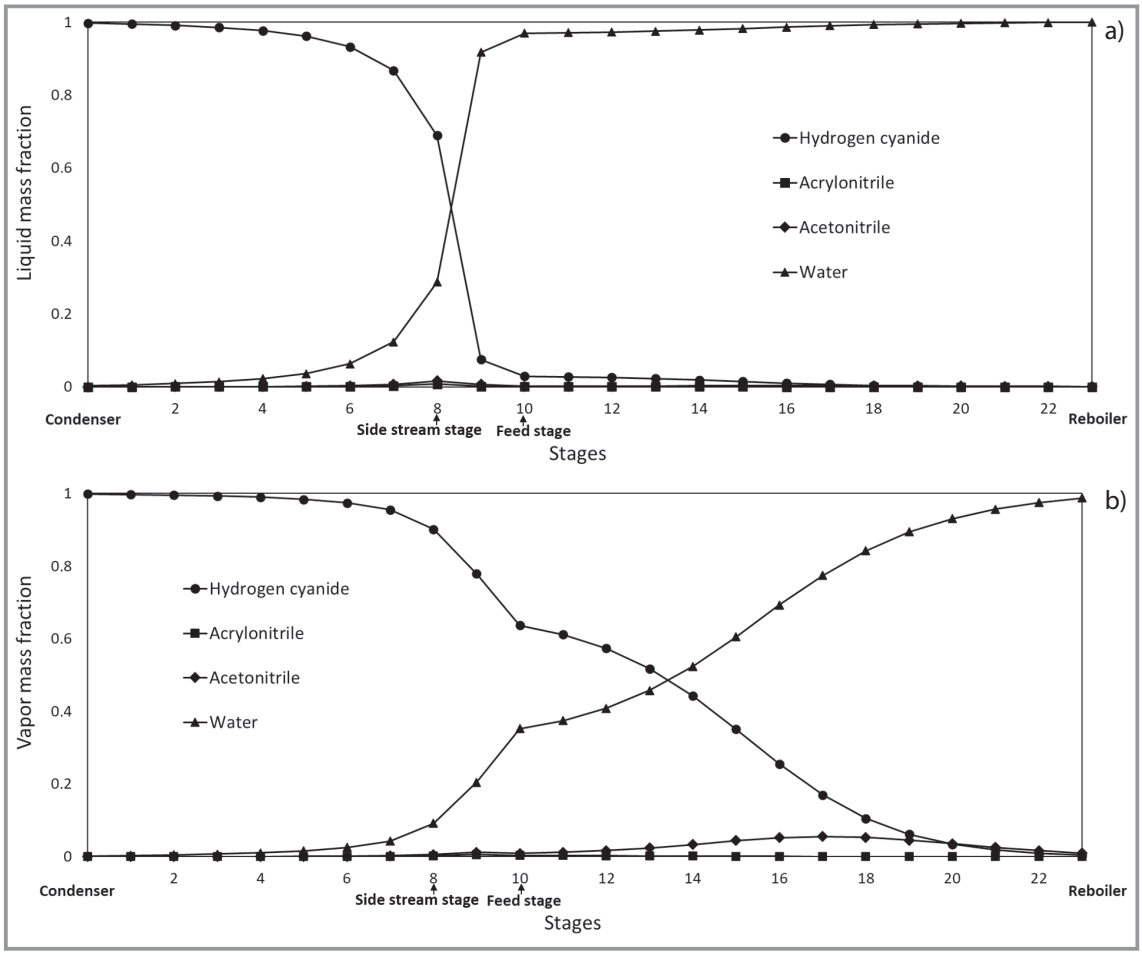

Figure 8. Component mass fraction profiles in the main column (the cost-optimal design of the base case) after the integration of a side stripper (column with a side stripper) for a) the liquid phase, b) the vapor phase, L_{ss} = 1700 kg h^{-1}, *NITRIWA* = 500 kg h^{-1}.

5.2 Heat Integration

A further step for process intensification of the distillation unit of the Andrussow process was carried out. For this purpose, the possibility of heat integration was examined in the distillation process with the design configuration developed in the previous section (column with a side stripper). It was found that using the bottom product of the main column (WASTWAT) as heating medium for feed preheating, instead of lp-steam constitutes a good solution for energy savings. Tab. 10 summarizes the design parameters obtained for the heat exchanger used for feed preheating by means of the bottom product of the main column as hot stream. Fig. 9 shows the final obtained process flow diagram including heat integration. As expected, Tab. 11 shows that the intensification approach presented in this work for the distillation unit of the Andrussow process allows not only to address the operational issues of the process due to presence of organonitrile contaminants in the feed but permits also a considerable energy savings; leading therefore to a reduction of *TAC* by 61 % as compared to the design of the base case.

Table 10. Design parameters of the heat exchanger used for feed preheating by heat integration.

Parameter	Value
Heater (heating medium: stream WASTWAT)	
Inlet temperature hot stream (WASTWAT) [°C]	99.8
Inlet / outlet temperature cold stream (Feed) [°C]	20/75
A_{hex} [m^2]	400.46
Material of construction	Stainless steel 1.4301, AISI 304

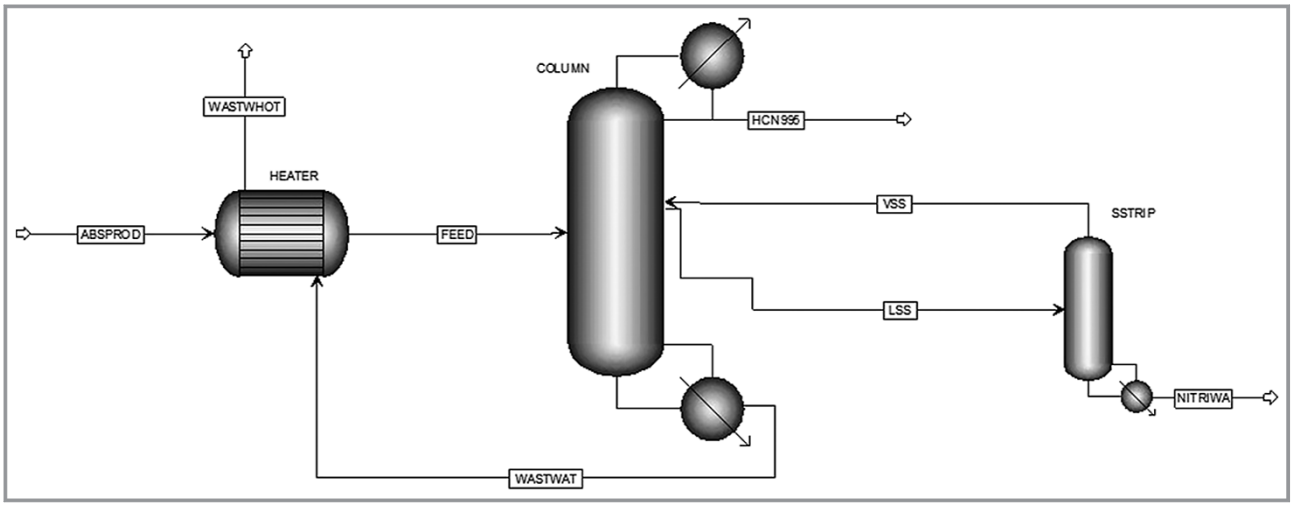

Figure 9. Heat integration in the new design of the distillation unit of the Andrussow process (with integrated side stripper) using the bottom product as hot stream for feed preheating.

Table 11. Costs of the new established cost-optimal design configuration of the distillation unit of the Andrussow process (cost-optimal base case with integrated side stripper including heat integration for feed preheating).

Costs	
Annual utility costs [€ a^{-1}]	2 164 682
Capital costs [€]	3 172 401
Total annual costs [€ a^{-1}]	3 222 148

6 Conclusions

In this work, investigations have been carried out to examine the influence of the presence of organonitrile contaminants in the feed on the operation (among other the risk of polymerization, foaming and column overloading) and on the performance (product qualities) of the distillation unit of the Andrussow process. Based on these studies, an approach for a cost-optimal process intensification was developed with the goal to achieve the desired product qualities, while minimizing the organonitrile build-up in the column. For this purpose, the established cost-optimal design of the base case was extended to a column with a side stripper. Furthermore, a heat integration concept was applied in the process by using the bottom product of the main column as hot stream for feed preheating. It was found that this configuration allows a considerable minimization of the accumulation of organonitriles in the main column; diminishing thereby the operation issues in the process. Finally, as compared to the design of the base case, the new established design permits important energy savings with a reduction of the *TAC* by 61 %.

Supporting Information

Supporting Information for this article can be found under DOI: https://doi.org/10.1002/cite.202200059. This section includes (i) thermodynamic phase equilibrium curves of the system HCN-water obtained by the regressed NRTL model established in this work, (ii) data and correlations of the cost model of the distillation unit of the Andrussow process and (iii) results of sensitivity analysis for the design optimization of the column with a side stripper.

Acknowledgment

Open access funding enabled and organized by Projekt DEAL.

Symbols used

A_{cond}	[m^2]	heat exchange area of condenser
A_{hex}	[m^2]	heat exchange area of feed preheater
$A_{reb,mc}$	[m^2]	heat exchange area of the reboiler of the main column
$A_{reb,ss}$	[m^2]	heat exchange area of the reboiler of the side stripper
$C_{cw/j}$	[€ J^{-1}]	price of chilled water
$C_{lps/j}$	[€ J^{-1}]	price of low-pressure steam
ΔH_R	[kJ mol^{-1}]	heat of reaction
N_F	[–]	optimal feed stage
Q_{cond}	[J s^{-1}]	condenser heat duty
Q_{reb}	[J s^{-1}]	heat duty of all column reboilers of the distillation unit
$Q_{reb,mc}$	[J s^{-1}]	heat duty of the reboiler of the main column

$Q_{reb,ss}$	[J s^{-1}]	heat duty of the reboiler of the side stripper
Q_{hex}	[J s^{-1}]	heat duty of the feed preheater

References

[1] L. Andrussow, *Angew. Chem.* **1935**, *48 (37)*, 593–595.
[2] L. Andrussow, *Chem. Ing. Tech.* **1955**, *27 (8/9)*, 469–472. DOI: https://doi.org/10.1002/cite.330270804
[3] E. Gail, S. Gos, R. Kulzer, J. Lorösch, A. Rubo, M. Sauer, in *Ullmann's Encyclopedia of Industrial Chemistry*, Wiley-VCH, Weinheim **2012**.
[4] C. T. Kautter, W. Leitenberger, *Chem. Ing. Tech.* **1953**, *25 (12)*, 697–768. DOI: https://doi.org/10.1002/cite.330251202
[5] J. M. Pirie, *Platinum Metals Rev.* **1958**, *2 (1)*, 7–11.
[6] S. Forsyth, A. Liu, M. Renner, B. Stahlmann, *Patent WO 2014/099613 A1*, **2014**.
[7] W. D. Parten, R. O. Dixon, M. Bowford, G. R. Maxwell, S. L. Grise, *Patent WO 2017/011428*, **2017**.
[8] J. Edwards, J. Newman, J. M. Prausnitz, *AIChE J.* **1975**, *21 (2)*, 248–257. https://doi.org/10.1002/aic.690210205
[9] M. A. Opykhtina, O. T. Frost, *Zh. Obshch. Khim.* **1936**, *6*, 1778.
[10] S. Han, *Huaxue Gongcheng* **1980**, 22.
[11] J. Acosta, A. Arce, E. Rodil, A. Soto, *Fluid Phase Equilib.* **2002**, *203*, 83–98.
[12] N. M. Sokolov, N. N. Sevryugova, N. M. Zhavoronkov, *Khim. Prom-st. (Moscow)* **1967**, *43*, 776–779.
[13] N. M. Sokolov, N. N. Sevryugova, N. M. Zhavoronkov, *Zh. Fiz. Khim.* **1966**, *40*, 1086.
[14] W. Jiang, Y. Zhang, M. Cao, S.-J. Han, *Zhejiang Daxue Xuebao* **1983**, *3*, 25–41.
[15] *Perry's Chemical Engineers' Handbook* (Eds: D. W. Green), 8th ed., McGraw-Hill, New York **2007**.
[16] www.teamedelstahl.de/werkstoffe/1-4301/ (Accessed on May 10, 2022)
[17] H. Z. Kister, *Distillation Design*, McGraw-Hill, New York **1997**.
[18] J. M. Douglas, *Conceptual Design of Chemical Processes*, McGraw-Hill, New York **1988**.
[19] J. R. Couper, W. R. Penny, J. R. Fair, S. M. Walas, *Chemical Process Equipment: Selection and Design*, 2nd ed., Elsevier, Amsterdam **2005**.
[20] W. L. Luyben, *Distillation Design and Control using Aspen TM Simulation*, John Wiley & Sons, Hoboken, NJ **2006**.
[21] C. Adiche, B. Ait Aissa, *Chem. Eng. Res. Des.* **2016**, *109*, 150–170. DOI: https://doi.org/10.1016/j.cherd.2016.01.015
[22] C. Adiche, B. Ait Aissa, Rapid Evaluation of Distillation Process Alternatives Involving Complex Column Configurations for the Separation of Multicomponent Azeotropic Mixtures, *AIChE Annual Meeting Proceedings*, San Francisco, CA **2016**.
[23] www.sulzer.com/en/shared/products/mellapak-and-mellapakplus (Accessed on May 10, 2022)

